The Journal of Immunology

Polyethylene Glycol-Modified GM-CSF Expands CD11b ^{high}CD11c^{high} But Not CD11b ^{low}CD11c^{high} Murine Dendritic Cells In Vivo: A Comparative Analysis with Flt3 Ligand

Elizabeth Daro, Bali Pulendran, Kenneth Brasel, Mark Teepe, Dean Pettit, David H. Lynch, David Vremec, Lorraine Robb, Ken Shortman, Hilary J. McKenna, Charles R. Maliszewski and Eugene Maraskovsky

J Immunol 2000; 165:49-58; ;
doi: 10.4049/jimmunol.165.1.49
http://www.jimmunol.org/content/165/1/49

The Journal of Immunology is published twice each month by
The American Association of Immunologists, Inc.,
1451 Rockville Pike, Suite 650, Rockville, MD 20852

Print ISSN: 0022-1767 Online ISSN: 1550-6606.

Polyethylene Glycol-Modified GM-CSF Expands $CD11b^{high}CD11c^{high}$ But Not $CD11b^{low}CD11c^{high}$ Murine Dendritic Cells In Vivo: A Comparative Analysis with Flt3 Ligand

Elizabeth Daro,[1]* Bali Pulendran,[2†] Kenneth Brasel,* Mark Teepe,* Dean Pettit,[‡] David H. Lynch,* David Vremec,[§] Lorraine Robb,[§] Ken Shortman,[§] Hilary J. McKenna,* Charles R. Maliszewski,[†] and Eugene Maraskovsky[3]*

Dendritic cells (DC) are potent APCs that can be characterized in the murine spleen as $CD11b^{high}CD11c^{high}$ or $CD11b^{low}CD11c^{high}$. Daily injection of mice of Flt3 ligand (FL) into mice transiently expands both subsets of DC in vivo, but the effect of administration of GM-CSF on the expansion of DC in vivo is not well defined. To gain further insight into the role of GM-CSF in DC development and function in vivo, we treated mice with polyethylene glycol-modified GM-CSF (pGM-CSF) which has an increased half-life in vivo. Administration of pGM-CSF to mice for 5 days led to a 5- to 10-fold expansion of $CD11b^{high}CD11c^{high}$ but not $CD11b^{low}CD11c^{high}$ DC. DC from pGM-CSF-treated mice captured and processed Ag more efficiently than DC from FL-treated mice. Although both FL- and pGM-CSF-generated $CD11b^{high}CD11c^{high}$ DC were $CD8\alpha^-$, a greater proportion of these DC from pGM-CSF-treated mice were $33D1^+$ than from FL-treated mice. $CD11b^{low}CD11c^{high}$ DC from FL-treated mice expressed high levels of intracellular MHC class II. DC from both pGM-CSF- and FL-treated mice expressed high levels of surface class II, low levels of the costimulatory molecules CD40, CD80, and CD86 and were equally efficient at stimulating allogeneic and Ag-specific T cell proliferation in vitro. The data demonstrate that treatment with pGM-CSF in vivo preferentially expands $CD11b^{high}CD11c^{high}$ DC that share phenotypic and functional characteristics with FL-generated $CD11b^{high}CD11c^{high}$ DC but can be distinguished from FL-generated DC on the basis of Ag capture and surface expression of 33D1. ***The Journal of Immunology,*** **2000, 165: 49–58.**

Dendritic cells (DC)[4] are rare, but widely distributed, hemopoietic cells that form a cellular network involved in immune surveillance and the induction of immune responses (1). DC acquire Ags in peripheral tissues, migrate to lymphoid organs, and present these Ags, as processed peptides, in the context of MHC molecules to T cells, leading to the development of Ag-specific immunity (1–3). Immature DC found in peripheral tissues are characterized by high Ag capture capacity, high intracellular MHC class II, and low expression of costimulatory molecules such as CD80 and CD86. Stimuli such as epithelial barrier breakdown, pathogens, and inflammatory mediators cause DC to mature and migrate to lymphoid tissues. On DC maturation, Ag-capturing activity is down-regulated, surface expression of costimulatory molecules is up-regulated, and class II molecules are translocated from intracellular compartments to the cell surface. Thus, immature DC are specialized for capturing Ag in peripheral tissues, whereas mature DC are specialized for highly efficient Ag presentation to effector T cells in the lymphoid tissues (4–8).

Although GM-CSF is an important cytokine for the generation of myeloid-related DC in vitro, the role of this cytokine in vivo has been less well defined. Examination of mice deficient in GM-CSF or in GM-CSFRβ indicates that DC development in lymphoid tissue is not dramatically affected (9). Similarly, DC numbers are not increased in GM-CSF-transgenic mice, except in the peritoneal cavity (10). Additionally, in one study, systemic administration of unmodified yeast-derived murine GM-CSF into mice did not significantly increase the numbers of DC in the spleen, peripheral blood (PB), or lymph nodes (LN) (11). However, several other studies indicate that GM-CSF is capable of modulating immune responses in vivo. Transplantation of tumors transduced with GM-CSF results in the expansion of DC in vivo (12, 13) and the generation of antitumor immune responses (14, 15). Similarly, transduction of DC with GM-CSF enhances their Ag-presenting functions in vivo (16). We recently reported that treatment of mice in vivo with a polyethylene glycol (PEG)-modified form of yeast-derived murine GM-CSF (pGM-CSF) expands the number of $CD11b^{high}CD11c^{high}$ but not $CD11b^{low}CD11c^{high}$ DC in murine spleen (17). PEG-modified proteins are more resistant to hepatic clearance and therefore have a more stable and prolonged biological half-life in vivo (18).

In contrast to GM-CSF, the role of the hemopoietic growth factor Flt3 ligand (FL) in the expansion of DC has been better defined in vivo than in vitro. FL increases the numbers of both $CD11b^{high}$ $CD11c^{high}$ and $CD11b^{low}CD11c^{high}$ DC when administered to mice

Departments of *Immunobiology, [†]Research Administration, and [‡]Analytical Chemistry and Formulation, Immunex Corporation, Seattle, WA 98101; and [§]The Walter and Eliza Hall Institute of Medical Research, Melbourne, Australia

Received for publication October 8, 1999. Accepted for publication April 12, 2000.

The costs of publication of this article were defrayed in part by the payment of page charges. This article must therefore be hereby marked *advertisement* in accordance with 18 U.S.C. Section 1734 solely to indicate this fact.

[1] Address correspondence and reprint requests to Dr. Elizabeth Daro, Department of Immunobiology, Immunex Corporation, 51 University Street, Seattle, WA 98101.

[2] Current address: Baylor Institute of Immunology Research, Dallas, TX.

[3] Current address: Ludwig Institute for Cancer Research, Melbourne, Australia.

[4] Abbreviations used in this paper: DC, dendritic cells; PB, peripheral blood; LN, lymph nodes; PEG, polyethylene glycol; pGM-CSF, PEG-modified GM-CSF; FL, Flt3 ligand; BM, bone marrow; MFI, mean fluorescence intensity.

0022-1767/00/$02.00

in vivo (11, 19, 20). In addition, administration of FL to humans results in transient DC expansion (51). FL-deficient mice exhibit markedly reduced numbers of both $CD11b^{high}CD11c^{high}$ and $CD11b^{low}CD11c^{high}$ DC (52).

In this study, we have taken advantage of the increased half-life of pGM-CSF to gain further insight into the role of this cytokine in DC development and function. To this end, we have compared DC generated by daily administration of pGM-CSF or FL to mice. With regard to DC development, pGM-CSF preferentially expanded $CD11b^{high}CD11c^{high}$ but not $CD11b^{low}CD11c^{high}$ DC. The pGM-CSF- and FL-generated, $CD11b^{high}CD11c^{high}$ DC expressed similar levels of MHC class II, CD40, CD80, and CD86 but expression of 33D1 was more homogeneous in pGM-CSF-generated $CD11b^{high}CD11c^{high}$ DC than in FL-generated $CD11b^{high}CD11c^{high}$ DC. Functionally, pGM-CSF-generated DC captured and processed Ag more efficiently than FL-generated DC but were equally efficient at stimulating T cell proliferation in vitro. The data highlight the role of pGM-CSF in the development of DC that are functionally and phenotypically similar to but distinct from FL-generated DC.

Materials and Methods

Mice and cytokine treatment protocols

Female C57BL/6, DBA/2, and BALB/c mice were obtained from The Jackson Laboratory (Bar Harbor, ME) or Taconic (Germantown, NY). DO11.10 mice (21) were kindly provided by Dr. Mark Jenkins and GM-CSFR$\beta^{-/-}$ mice (22) were bred and maintained at Immunex and the Walter and Eliza Hall Institute, respectively. All mice used were 6–10 wk old and were maintained in specific pathogen-free facilities. The status of the GM-CSFRβ chain genes was determined by RT-PCR analysis of tail DNA. Mice (three to five per group) were injected once daily (s.c. at the nape of the neck) with 10 μg recombinant human FL (Chinese hamster ovary cell derived) for 9 consecutive days or 5 μg of either PEG-modified or unmodified murine GM-CSF for 5 consecutive days. PBS was used in control injections. FL and GM-CSF were produced at Immunex.

Preparation of pGM-CSF

Recombinant murine GM-CSF was produced in yeast (*Saccharomyces cerevisiae*) as described (23). N-terminal PEG conjugation was conducted with 20-kDa PEG that was obtained in the activated form of succinimidylpropionic acid PEG (Shearwater Polymers, Huntsville, AL). A 6-fold molar excess of succinimidylpropionic acid PEG was added to a solution of murine GM-CSF in 20 mM NaH_2PO_4, 50 mM cyanoborohydride (pH 6.0), and the reaction was allowed to proceed overnight at 2–8°C. Mono-PEG-conjugated murine GM-CSF was purified from the reaction mixture by anion exchange chromatography with Q Sepharose high performance resin (Pharmacia, Uppsala, Sweden) using a 0–150 mM NaCl elution gradient on a Perceptive Integral HPLC system. Purified protein solutions were concentrated and buffer exchanged into PBS. PEG-murine GM-CSF was then tested for endotoxin levels, by the LAL method, and total protein concentration was determined by amino acid analysis.

Pharmacokinetics of native and pGM-CSF

Pharmacokinetic parameters for native murine GM-CSF and pGM-CSF were determined from blood concentration/time profiles essentially as described (24). Briefly, after i.v. injection, mice were bled at various time points ranging from 1 min to 24 h, and serum GM-CSF concentration was determined by bioassay or radioassay. The bioassay was performed by titrating serum samples onto the GM-CSF-responsive cell line, FDCP2.1D and measuring [^{3}H]thymidine incorporation. ^{125}I iodination was used for the radioassay, and the serum was TCA precipitated before gamma counting. The apparent elimination rate constant (K) and the half-life ($t_{1/2}$) were calculated using a pharmacokinetic half-life program on an RS/1 system. The log linear portion of the concentration/time curve was used to calculate K with $t_{1/2}$ determined as $t_{1/2} = \ln 2/K$. Half-life values are presented as $t_{1/2}$ SE, where SE indicates the error in fitting the log linear line to the data points in calculating the K value. The distribution ($t_{1/2}\alpha$) and elimination ($t_{1/2}\beta$) half-lives were calculated using a biphasic pharmacokinetics program that related the respective log linear concentration/time curves to specific K and $t_{½}$ values. The area under the blood concentration/time curve from $t = 0$ to infinite time was determined by conventional trapezoidal summation and extrapolation.

Antibodies

All Abs were from PharMingen (San Diego, CA) except DEC205 (NLDC-145; a gift from Dr. G. Kraal, Free University, Amsterdam, The Netherlands) and 33D1 (hybridoma from the American Type Culture Collection (Manassas, VA), produced and biotinylated at Immunex). The following clones were used unless otherwise noted: CD1d (1B1); CD3 (17A2); CD4 (L3T4); CD8α (53-6.7); CD11b (M1/70); CD11c (HL3); CD19 (1D3); CD40 (3/23); CD80 (16-10A1); CD86 (GL1); B220 (RA36B2); GR-1 (RB6−8C5); H-2Kb (AF6-88.5); I-Ab (AF6-120.1); NK1.1 (PK136); TER-119 (TER119); and Thy-1.2 (T24).

Phenotyping of DC

Phenotyping of the various populations was performed by incubating cells with either FITC-, APC-, or PE-conjugated Ab or biotinylated Ab which were detected with APC-conjugated streptavidin. Flow cytometry was performed using a FACScalibur (Becton Dickinson, San Jose, CA) and results were analyzed with Cellquest software (Becton Dickinson).

Isolation of DC

Spleens were removed from control, FL-, or pGM-CSF-treated mice and single-cell suspensions were prepared and depleted of erythrocytes with NH_4Cl. Thymus and LN (inguinal and axillary) were also harvested from GM-CSFR$\beta^{-/-}$ and GM-CSFR$\beta^{+/+}$ mice. The various cell suspensions were incubated with Ab to Thy-1.1, B220, NK1.1, Gr-1 and Ter-119 for 30 min at 4°C. The cells were then centrifuged and resuspended. mAb-coated cells were removed using anti-Ig-coated magnetic beads (Dynabeads, Dynal, Oslo, Norway). The enriched cells were incubated with FITC-conjugated anti-CD11c, and PE-conjugated anti-CD11b and the various cell populations were then isolated by flow cytometry using a FACStar^{Plus} (Becton Dickinson) or a EPICS Elite (Coulter, Brea, CA) cell sorter.

Measurement of Ag uptake

Cells were harvested from spleen, PB, or bone marrow (BM) of mice treated with FL or pGM-CSF as described above. After incubation with FITC-dextran (70 kDa), FITC-OVA, or FITC-zymosan (Molecular Probes, Eugene, OR) at 37°C, cells were washed three times in PBS-5% FBS and then incubated with PE-anti-CD11c and APC-anti-CD11b. Flow cytometry analysis of CD11b and CD11c identified DC subpopulations. FITC-dextran, FITC OVA, or FITC-zymosan uptake was quantified as mean fluorescence intensity (MFI). Nonspecific FITC signal was assessed by incubating cells in FITC-dextran, -OVA, or -zymosan at 0°C. For time course of uptake, cells were incubated with 2 mg/ml FITC-dextran or FITC-OVA for 0–90 min. For dextran or OVA titration, cells were incubated with 0.001–5.0 mg/ml for 30 min at 37°C. Phagocytosis was assessed by incubating cells with 1 mg/ml FITC-zymosan for 90 min at 37°C. In some conditions, cells were pretreated with 10 μM cytochalasin D (Sigma, St. Louis, MO) for 30 min at 37°C to depolymerize actin. All incubations were performed in PBS-5% FBS. To verify that the flow cytometry-based FITC signal represented internalized dextran, OVA, or zymosan, cells were analyzed by epifluorescence and phase-contrast microscopy.

Intracellular distribution of MHC class II

DC were isolated by flow cytometry as described above, except APC-conjugated CD11b and biotinylated CD11c followed by Texas Red-streptavidin (Molecular Probes) were used to identify DC populations. Sorted DC were plated onto fibronectin-like polymer (Sigma)-coated coverslips and incubated for 30 min at 37°C in DMEM, 10% FBS, 900 μM Ca^{2+}, 500 μM Mg^{2+}. After fixation in 4% paraformaldehyde, cells were permeabilized and blocked with PBS, 0.1% saponin (Sigma), 10% FBS. Intracellular and cell surface MHC class II were detected by incubation with FITC-conjugated anti-I-A^b Ab (Boeringer Ingelheim clone M5-114) in PBS, 0.1% saponin, 10% FBS. The coverslips were gently washed three times in PBS, 0.1% saponin, 10% FBS; once in PBS; and once in double-distilled H_2O and were mounted in Moviol (Calbiochem, La Jolla, CA) containing 2.5% 1,4-diazabicyclo[2.2.2]octane (Sigma) on glass slides. MHC class II distribution was analyzed by confocal microscopy in 0.75-μm sections on a Bio-Rad 1024 confocal head (Bio-Rad, Richmond, CA; outfitted with a

Table I. *Treatment with pGM-CSF in vivo expands myeloid cells in murine spleen, bone marrow, and blood*[a]

	% Cells								Total Cells ($\times 10^{-6}$)					
	SP		LN		PB		BM		Cells/SP		Cells/4LN		Cells/ml PB	
	C	GM	C	GM	C	GM	C	GM	C	GM	C	GM	C	GM
$CD11b^+/GR\text{-}1^+$	2.5 ± 0.3	29.0 ± 8.3	ND	ND	8.6	49.0	33.0	80.4	3.8 ± 0.8	101.0 ± 35.8	ND	ND	0.3	6.8
$CD11b^+/CD11c^+$	2.1 ± 0.2	11.0 ± 2.8	1.0	3.6	1.6	3.7	1.7	1.3	3.2 ± 0.6	37.4 ± 9.5	0.2	2.8	0.1	0.5
$CD11b^-/CD11c^+$	2.9 ± 0.5	1.8 ± 0.3	0.7	1.7	1.4	0.3	2.0	ND	4.3 ± 1.0	6.2 ± 1.0	0.2	1.3	0.1	0.0
$B220^+/CD19^+$	49.1 ± 4.9	18.8 ± 2.2	40.0	40.0	53.0	24.0	20.0	1.5	74.7 ± 21.3	63.4 ± 3.0	9.9	30.9	2.0	3.3
$CD3^+$	33.9 ± 3.1	23.8 ± 2.7	59.0	53.0	23.0	15.0	ND	ND	51.6 ± 12.4	80.4 ± 4.4	14.6	40.9	0.9	2.1
$NK1.1^+$	5.7 ± 0.3	4.1 ± 2.7	1.1	1.7	11.0	4.0	ND	ND	8.7 ± 1.5	13.5 ± 7.9	0.3	1.3	0.4	0.6
$TER\text{-}119^+$	4.0 ± 1.4	18.9 ± 6.4	ND	ND	1.1	0.4	ND	ND	6.1 ± 1.2	63.7 ± 18.9	ND	ND	0.0	0.1
Total	100.3 ± 2.2	107.0 ± 6.2	101.8	100.0	99.7	96.4	56.7	83.2	152.4 ± 35.0	365 ± 24.9	25.2	77.2	3.8	13.3

[a] Cells were isolated and counted from spleens (SP), LN (pooled axillary and inguinal), PB, and BM of PBS (control, C)- or pGM-CSF (GM)-treated mice (5 μg/mouse/day for 5 days). Cells were analyzed for surface expression of various markers of B cells (B220, CD19), T cells (CD3), NK cells (NK 1.1), DC (CD11b, CD11c), myeloid cells (GR-1), and erythroid cells (TER-119). ND, no data. For spleens, data represent the mean ± SD ($n = 4$). For other tissues, data represent pooled cells from tissues of three mice per group.

Zeiss axiovert microscope (Zeiss, Oberkochen, Germany) using the 63× plan apochromat objective. Control cells that were labeled with only CD11b-APC or CD11c-TxR were used to ensure that there was no bleedthrough into the FITC-MHC class II channel from residual CD11b or CD11c after FACS sorting.

Flow cytometry-based quantification of MHC Class II distribution was determined by comparing permeabilized (total MHC class II) and nonpermeabilized (cell surface MHC class II) cells. Spleen cells isolated from FL- and pGM-CSF-treated mice were incubated with APC-CD11b and TxR-CD11c, washed, and fixed in 2% paraformaldehyde. The cells were incubated with FITC-conjugated anti-$I\text{-}A^b$ (AF6-120.1) in PBS, 5% FBS in the absence or presence of 0.1% saponin at 0°C for 30 min. The cells were washed three times in PBS, 5% FBS in the absence or presence of saponin and once in PBS and refixed in 2% paraformaldehyde. MHC class II distribution was determined by flow cytometry analysis and quantified as MFI for each population. Cell surface MHC class II was quantified using nonpermeabilized cells, and intracellular MHC class II was determined by subtracting surface MHC class II (nonpermeabilized cells) from total MHC class II (permeabilized cells).

Processing of OVA into peptide

Cells were pulsed with DQ-OVA (Molecular Probes) for 15 min at 37°C and then washed extensively with PBS, 5% FBS at 4°C. Cells were transferred to 37°C, and processing of OVA into peptide was assayed by increase in MFI over time. DC populations and DQ OVA were identified and quantified by flow cytometry as in Ag capture assays. DQ-conjugated OVA peptide was quantified using the FITC channel of a FACSCalibur (Becton Dickinson).

Preparation and purification of alloreactive and Ag-specific $CD4^+$ and $CD8^+$ T cells

$CD4^+$ or $CD8^+$ allogeneic T cells (90–95% pure) were isolated from the peripheral LN of 4- to 8-wk-old DBA/2 ($H\text{-}2^d$) mice. $CD4^+$-transgenic T cells were isolated from the inguinal LN, axillary LN and spleens of 8-wk-old OVA-TCR-transgenic DO11.10 ($H\text{-}2^d$) mice. LN cells were incubated with Abs to MHC class II ($I\text{-}A^b$ or $I\text{-}A^d$), B220, and either CD4 or CD8 and for 30 min at 4°C. Ab-coated cells were depleted with anti-Ig-coated magnetic beads (Dynabeads). Depleted LN cells were composed of at least 90% $CD4^+$ or $CD8^+$ T cells as determined by FACS analysis. Naive $CD4^+$-transgenic T cells were further purified by cell sorting on the basis of CD62L expression using a $FACStar^{Plus}$ (Becton Dickinson).

MLR and Ag-specific T cell assay

Assays were performed in 96-well round-bottom culture plates in 0.2 ml DMEM containing 10% FCS in humidified 10% CO_2 for 5 days. DC populations were isolated as above and irradiated with 2000 rad. In the MLR, purified, allogeneic $CD4^+$ or $CD8^+$ LN T cells (1×10^5) from DBA/2 mice ($H\text{-}2^d$) were cultured with 2×10^1–1×10^4 DC from either FL- or pGM-CSF-treated C57BL/6 mice ($H\text{-}2^b$). To detect Ag-specific presentation, purified $CD4^+CD62L^+$LN T cells (1×10^4) from DO11.10 mice were cultured in 96-well plates with 10^1–10^4 irradiated DC (2000 rad) from either FL- or pGM-CSF-treated syngeneic BALB/c mice. Cultures were conducted in the presence of a constant concentration of $OVA_{323–329}$ peptide (10 μg/ml) or protein (Sigma, 300 μg/ml) or with constant numbers of DC (1×10^4) in the presence of varying concentrations of $OVA_{323–329}$ peptide or protein in 0.2 ml culture medium for 5d. In GM-CSFR$\beta^{-/-}$ experiments, purified $CD4^+$ or $CD8^+$ LN T cells (2×10^4) from BALB/c ($H\text{-}2^d$) mice were cultured with 1.25×10^2–2×10^3 DC from GM-CSFR$\beta^{-/-}$ or GM-CSFR$\beta^{+/+}$ mice ($H\text{-}2^b$) for 6 days in 96-well V-bottom wells in HEPES-buffered RPMI 1640 supplemented with 10% FCS, 10^{-4} M 2-ME, and sodium pyruvate. The cultures were pulsed with 0.5 μCi [^{3}H]thymidine for 8 h, and the cells were harvested onto glass fiber sheets for counting on a gas-phase beta counter. The background counts for either T cells or DC cultured alone were <100 cpm.

Results

pGM-CSF has an increased half-life in mice

The in vivo pharmacokinetics of pGM-CSF was compared with that of unmodified, recombinant murine GM-CSF. After s.c. administration to mice, pGM-CSF was found to have a distribution half-life ($t_{1/2}\alpha$) of 15.9 ± 1.5 min and an elimination half-life ($t_{1/2}\beta$) of 5.3 h ± 13 min. In contrast, unmodified, recombinant murine GM-CSF had a $t_{1/2}\alpha$ of 0.92 ± 0.04 min and a $t_{1/2}\beta$ of 11.75 ± 3.89 min. Thus, modification of GM-CSF by PEG increased the $t_{1/2}\alpha$ by >15-fold and the $t_{1/2}\beta$ by >27-fold. Splenic weight increased from 0.079 ± 0.018 g to 0.206 ± 0.037 g after s.c. injection of 0 and 5 μg pGM-CSF/mouse/day for 5 days, respectively (not shown). These data were generated in six separate experiments using six different batches of pGM-CSF and two to three mice per group. Thus, the SD observed may be a reflection of batch-to-batch variation, possibly due to variations in the extent of PEG derivitization. In contrast to pGM-CSF, s.c. injection of unmodified GM-CSF at 5 μg/day for up to 7 days had no effect on either spleen weight or white blood cell counts.

Treatment of mice with pGM-CSF expands $CD11b^{high}CD11c^{high}$ but not $CD11b^{low}CD11c^{high}$ DC.

We first compared the effects of daily s.c. injection of pGM-CSF on cells in the spleen, bone marrow (BM), LN, and PB of mice. In the spleen, PB, and BM, we found a marked increase in the proportion of $CD11b^+$ cells with a concomitant decrease in the percent of B cells ($B220^+CD19^+$) (Table I). Enlarged LN in pGM-CSF-treated mice were characterized by increased numbers of T cells ($CD3^+$) and B cells ($B220^+CD19^+$), although the percentages of these populations were unaltered (Table I). To date, there is no clear evidence that pGM-CSF directly influences the expansion or development of this leukocyte compartment. This suggests that the effects in the lymph node are unlikely to be direct but may reflect changes in trafficking and retention of lymphocytes in the LN or a compensatory homeostatic feedback mechanism.

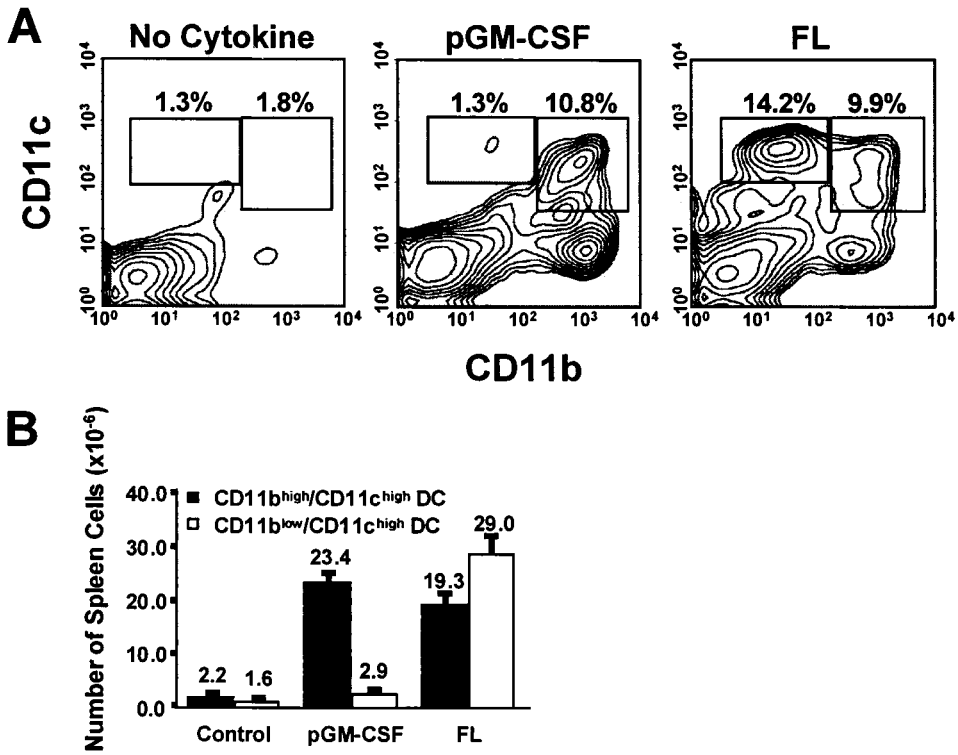

FIGURE 1. Treatment of mice with pGM-CSF expands CD11b^{high} CD11c^{high} DC but not CD11b^{low} CD11c^{high} DC. Mice were treated with PBS (control), pGM-CSF (5 μg/day/5 days), or FL (10 μg/day/10 days). Spleen cells were isolated and analyzed for expression of CD11b and CD11c. *A*, Flow cytometric analysis of spleen cells from mice treated with PBS, pGM-CSF, or FL. The profiles are representative of >10 independent experiments of 2 or more FL- or pGM-CSF-treated mice per experiment. *B*, Summary of the total numbers of DC subpopulations in the spleens of untreated, pGM-CSF-treated, and FL-treated mice. Data are presented as means ± SD for three replicates. Similar results were obtained on >10 separate occasions, but there was variance associated with different batches of pGM-CSF.

We next compared the capacity of pGM-CSF to generate DC in vivo to that of FL, a cytokine known to generate large numbers of CD11b^{high}CD11c^{high} and CD11b^{low}CD11c^{high} DC (11). Administration of pGM-CSF in vivo for 5 days increased the numbers of CD11b^{high}CD11c^{high} but not CD11b^{low}CD11c^{high} DC in the spleen, whereas FL expanded both CD11b^{high}CD11c^{high} and CD11b^{low}CD11c^{high} DC when administered to mice for 10 days (Fig. 1). Injection of pGM-CSF s.c. at 5 μg/mouse/day for 0–15 days revealed that maximal DC numbers were achieved at day 5 and dropped by 24 and 47% at days 9 and 15, respectively (not shown). In contrast, we have previously shown that a minimum of 9 days is required to achieve maximal numbers of DC after injection of Flt3L (11). The absolute number of splenic DC generated by pGM-CSF was 26.3×10^6 cells/spleen, 1.8-fold less than that generated after 9 days of treatment with FL (48.3×10^6 cells/spleen, Fig. 1*B*). In addition to the expansion of CD11b^{high}CD11c^{high} DC, pGM-CSF also expanded a population of CD11b^{high}CD11c^{low} cells (Fig. 1*A*), which were also positive for GR-1, and by morphology represented a mixture of relatively immature myeloid cells as well as granulocytes (not shown).

DC from pGM-CSF- and FL-treated mice express low levels of CD40, CD80, CD86, and high levels of MHC Class II

FL- and pGM-CSF-generated splenic DC expressed low levels of the costimulatory molecules, CD40, CD80, CD86, and relatively high levels of MHC class II (Fig. 2). We previously reported that FL-generated splenic DC express low levels of CD40 and CD86, negligible levels of CD80 and high levels of MHC class II (11, 20). Using a more sensitive anti-CD80 Ab (clone 16-10A1), we were able to detect low level expression of CD80 on FL-generated DC (Fig. 2).

DC from pGM-CSF-treated mice differ in expression of CD1d and 33D1

The majority of CD11b^{low}CD11c^{high} splenic DC from FL-treated mice expressed bright levels of CD8α and DEC205 (Fig. 2) (20).

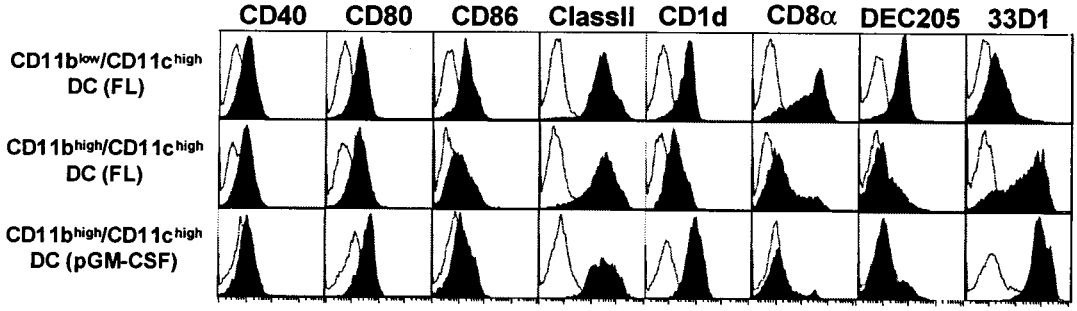

FIGURE 2. Comparison of surface phenotype of pGM-CSF- and FL-generated DC. Flow cytometric analysis of electronically gated DC populations as shown in Fig. 1*A* from the spleens of pGM-CSF- and FL-treated mice. Spleen cells were incubated with Ab to CD11c, CD11b, and one of the following: CD40 CD80, CD86, MHC Class II, CD1d, CD4, CD8α, DEC-205, or 33D1. Surface expression of these molecules is represented as filled histograms. Open histograms represent isotype controls.

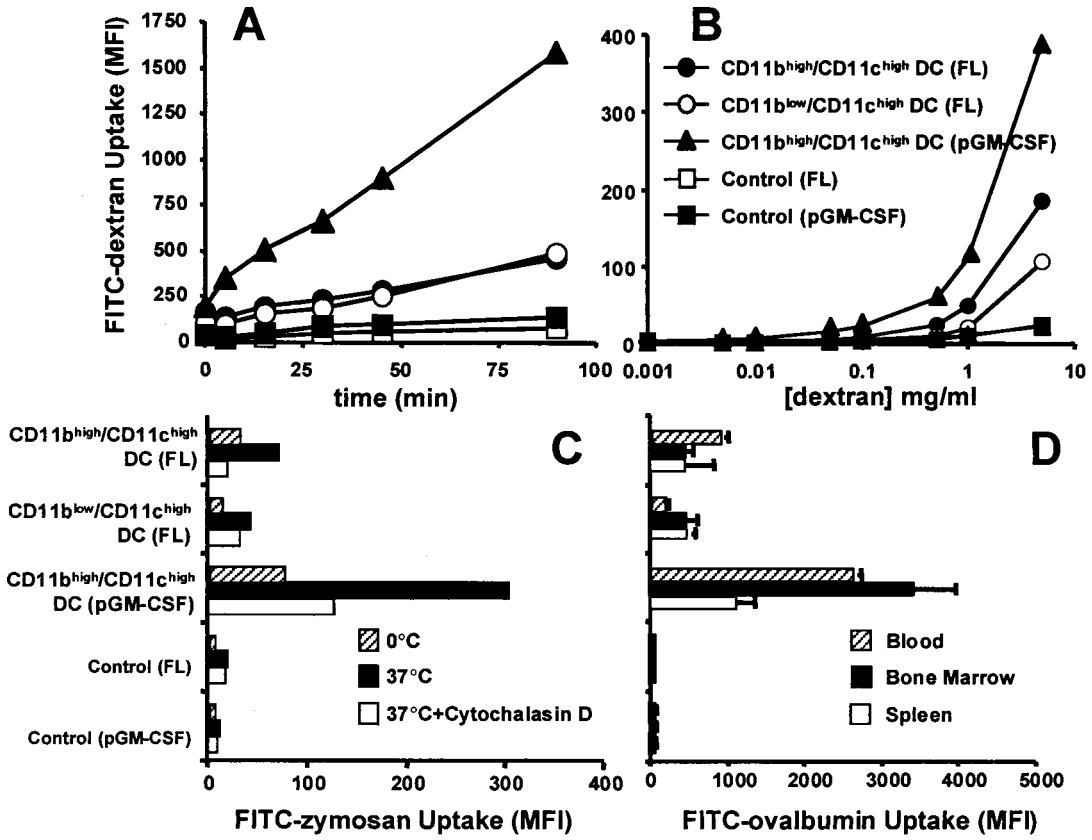

FIGURE 3. DC from pGM-CSF-treated mice capture Ag more efficiently than DC from FL-treated mice. Splenocytes were incubated with FITC-dextran-OVA, or Ovalbumin-zymosan. Cells were examined by flow cytometry to identify $CD11b^{low}CD11c^{high}$ DC, $CD11b^{high}CD11c^{high}$ DC, and the control cells ($CD11b^{-}CD11c^{-}$) and to assess internalized FITC. The data are presented as the MFI of internalized FITC. Each group represents pooled spleen cells from three mice unless otherwise noted. *A* and *B* share the same legend, and *C* and *D* share the same *y*-axis. *A*, Dextran internalization is 4-fold faster in pGM-CSF-generated DC. Cells were cultured with FITC-dextran for 0–90 min. Similar results were obtained on >10 separate occasions at 30 and 60 min of uptake. *B*, FITC-dextran uptake is not saturable. Cells were cultured with .001–5 mg/ml FITC-dextran for 30 min. *C*, Phagocytosis is enhanced in pGM-CSF-generated DC. Cells were incubated with FITC-zymosan particles for 90 min at 0°C or 37°C in the absence or presence of cytochalasin D. Cytochalasin D effectively inhibited the phagocytosis of zymosan. Data are representative of three separate experiments. *D*, ovalbumin uptake is maximal in DC generated from BM of pGM-CSF-treated mice. Cells were harvested from spleen, PB, and BM from six mice per group to give six separate samples for spleen and BM and pairs of peripheral blood samples were pooled to give three separate samples. Data are presented as means ± SD.

In contrast, the majority of $CD11b^{high}CD11c^{high}$ DC from FL-or pGM-CSF-treated mice did not express these markers (Fig. 2) (20). However, there were small proportions of $CD11b^{high}CD11c^{high}$ DC from FL- or pGM-CSF-treated mice that expressed $CD8\alpha$ or DEC205 (Fig. 2). The significance of these subpopulations of DC is unknown but may reflect DC that have been previously stimulated, because CD11b can be up-regulated on $CD8\alpha^{+}DEC205^{+}$ DC in vitro (25). $CD11b^{low}CD11c^{high}$ DC from FL-treated mice and $CD11b^{high}CD11c^{high}$ DC from pGM-CSF-treated mice expressed somewhat higher levels of CD1d than $CD11b^{high}CD11c^{high}$ DC from FL-treated mice (Fig. 2) (20). Whereas a large subpopulation of $CD11b^{high}CD11c^{high}$ DC from FL-treated mice expressed the marginal zone marker, 33D1 (Fig. 2) (20), virtually all of the $CD11b^{high}CD11c^{high}$ DC from pGM-CSF-treated mice expressed high levels of 33D1 (Fig. 2). These data demonstrate that pGM-CSF-generated $CD11b^{high}CD11c^{high}$ DC are not phenotypically identical with FL-generated $CD11b^{high}CD11c^{high}$ DC.

DC from pGM-CSF-treated mice capture Ag more efficiently than DC from FL-treated mice

DC capture a variety of Ags using several different mechanisms (reviewed in Ref. 26). Particulate Ags such as microbes and apoptotic cells can be internalized and degraded via the actin-dependent process of phagocytosis. Soluble Ags, such as proteins, can be internalized and degraded by actin-dependent macropinocytosis or clathrin-dependent endocytosis (including nonselective fluid phase endocytosis and receptor-mediated endocytosis). We therefore examined endocytosis and phagocytosis of splenic DC generated in vivo by treatment with FL or pGM-CSF. To assay the capture of soluble Ag, spleen cells from pGM-CSF- and FL-treated mice were incubated with 2 mg/ml FITC-dextran for 0–90 min. Analysis of various DC populations by FACS revealed that all DC populations were capable of internalizing soluble dextran, although the initial rate of internalization for pGM-CSF-generated DC was ~4-fold faster than that of FL-generated DC (Fig. 3*A*). The lymphocyte-enriched control population was inefficient at uptake of soluble FITC-dextran (Fig. 3*A*). Similar results were obtained using 2 mg/ml FITC-OVA (not shown).

Fluid-phase endocytosis is receptor independent (reviewed in Ref. 27). The capture of dextran was receptor independent because it was not saturable to 5 mg/ml (Fig. 3*B*). Similar results were obtained for OVA (not shown). Furthermore, the capture of dextran or OVA was not inhibited by the actin-depolymerizing agent cytochalasin D (not shown) and was not likely due to the actin-dependent process of macropinocytosis. Therefore, the enhanced

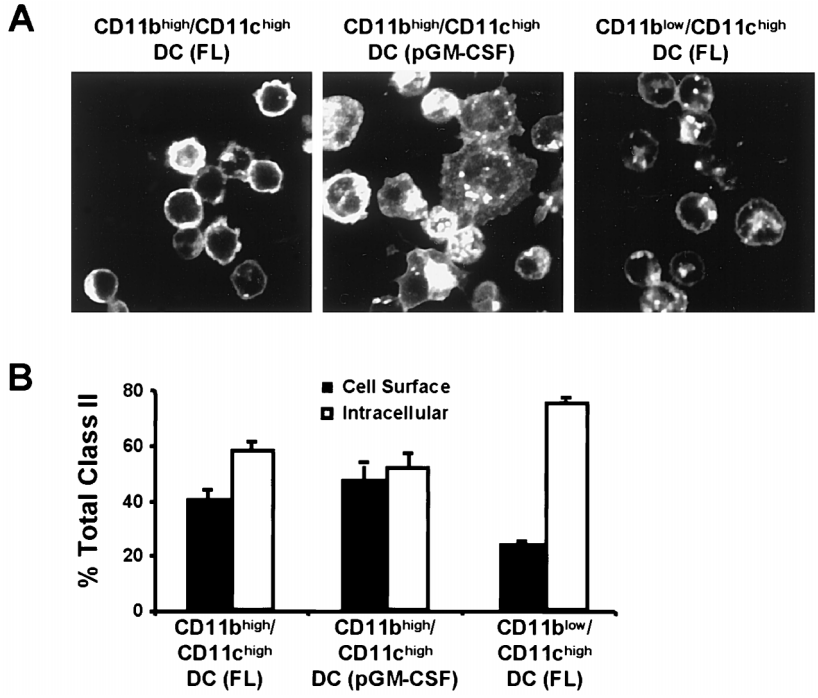

FIGURE 4. $CD11b^{low}CD11c^{high}$ DC from FL-treated mice have high intracellular MHC class II. *A*, Confocal microscopy of intracellular MHC class II. Splenic DC were isolated from FL- and pGM-CSF-treated mice and processed for intracellular MHC class II distribution. FL-generated, $CD11b^{high}CD11c^{high}$ DC expressed MHC class II on the cell surface (appears as a ring around the cell in confocal sections of spherical cells) and in intracellular vesicles (appear as puncta inside or near cell boundaries). pGM-CSF-generated, $CD11b^{high}CD11c^{high}$ DC also exhibited both cell surface staining (appears as a haze across the adherent surface of flat cells) and some intracellular vesicles. FL-generated, $CD11b^{low}CD11c^{high}$ DC contained many MHC class II positive intracellular vesicles. Sections are .75 μ and are taken in planes to reveal intracellular vesicles. *B*, Flow cytometry-based quantitation of MHC class II distribution. Cell surface MHC class II was quantified using nonpermeabilized cells, and intracellular MHC class II was determined by subtracting cell surface MHC class II (nonpermeabilized cells) from total MHC class II (permeabilized cells). Data are presented as mean percent total MHC class II ± SD; n = 3 replicates.

capture of soluble Ag observed in pGM-CSF-generated DC was due primarily to fluid-phase endocytosis and not macropinocytosis or receptor-mediated endocytosis.

Phagocytosis was also examined in the FL- and pGM-CSF-generated splenic DC by incubating DC with FITC-conjugated, yeast-derived zymosan particles for 90 min in the presence or absence of cytochalasin D. DC generated in vivo with pGM-CSF internalized ~5-fold more zymosan than DC generated in vivo with FL (Fig. 3*C*). Zymosan internalization was indeed due to actin-dependent phagocytosis because treatment with cytochalasin D was inhibitory (Fig. 3*C*). The control, lymphocyte-enriched populations were inefficient at phagocytosis (Fig. 3*C*).

Having determined that DC from the spleens of pGM-CSF-treated mice exhibit enhanced Ag capture efficiency, Ag capture potential was examined in DC from PB and BM, tissues that are more clinically accessible than the spleen. Uptake of FITC-OVA was enhanced in DC from PB, BM, and spleens of pGM-CSF-treated mice as compared with DC from FL-treated mice (Fig. 3*D*). Interestingly, DC from BM and PB of pGM-CSF-treated mice were more efficient at Ag capture than splenic DC (Fig. 3*D*). In contrast, FL-generated DC, including those from the BM, were relatively poor at Ag capture (Fig. 3*D*). Similar results were obtained for FITC-dextran uptake (not shown). Uptake was low in control lymphocyte-enriched populations from all tissues analyzed (Fig. 3*D*).

$CD11b^{low}CD11c^{high}$ DC from FL-treated mice have high levels of intracellular MHC class II

Intracellular class II can be detected in immature DC (reviewed in Ref. 4). We therefore examined the intracellular distribution of MHC class II. Splenic DC from mice treated with FL or pGM-CSF were isolated by flow cytometry and processed for intracellular MHC class II ($I\text{-}A^b$) localization. Confocal microscopy revealed that FL- and pGM-CSF-generated $CD11b^{high}CD11c^{high}$ DC expressed MHC class II on the cell surface and in intracellular vesicles (Fig. 4*A*). FL-generated, $CD11b^{low}CD11c^{high}$ DC exhibited a much higher proportion of MHC class II-containing intracellular vesicles compared with cell-surface MHC class II (Fig. 4*A*). Freshly isolated DC generated by pGM-CSF treatment are more adherent than those generated by FL treatment, and this results in greater cell spreading during the 30-min incubation. Thus, pGM-CSF-generated DC appear larger in Fig. 4*A*, but forward scatter analysis as well as cell volume comparisons using Cell-Tracker dye (Molecular Probes) showed no difference in cell size or volume between FL- and pGM-CSF-generated freshly isolated splenic DC in suspension. Quantification of intracellular MHC class II confirmed that FL-generated, $CD11b^{low}CD11c^{high}$ DC have higher levels of intracellular MHC class II than FL- or pGM-CSF-generated, $CD11b^{high}CD11c^{high}$ DC (Fig. 4*B*). FL- and pGM-CSF-generated $CD11b^{high}CD11c^{high}$ DC contained approximately equal amounts of intracellular and surface MHC Class II (Fig. 4*B*).

DC from pGM-CSF-treated mice process Ag more efficiently than DC from FL-treated mice

Processing of protein Ag into peptide is required for efficient presentation on MHC class II. Efficient internalization of extracellular Ags does not necessarily lead to delivery to an intracellular compartment where proteolysis occurs. We therefore assessed the capacity for the DC subsets to process internalized OVA into peptide. This was accomplished using DQ-OVA (Molecular Probes), a self-quenching conjugate designed specifically for the study of Ag processing. On proteolysis, highly fluorescent peptides are released from DQ-OVA, and thus processing of OVA into peptide can be quantified by flow cytometry. Spleen cells from pGM-CSF- and FL-treated mice were pulsed with 2 mg/ml DQ-OVA and chased for various amounts of time to allow protein processing. During the pulse period, pGM-CSF-generated DC internalized the most DQ-OVA because they are more efficient at capturing Ag (Fig. 5). However, the rate of OVA processing within the first 30 min (slope of the line between 0 and 30 min) was ~3-fold higher by the pGM-CSF-generated than that of FL-generated DC (Fig. 5). Thus, FL- and pGM-CSF-generated DC are capable of delivering internalized OVA to an intracellular compartment where proteolysis occurs.

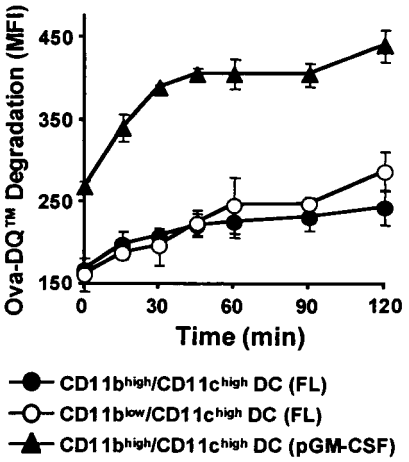

FIGURE 5. DC from pGM-CSF-treated mice process Ag more efficiently than DC from FL-treated mice. Cells were pulsed with DQ-OVA for 15 min and then washed extensively. Processing of DQ-OVA protein into peptide was then assayed by increase in fluorescence intensity over time at 37°C. DC populations and DQ-OVA were identified and quantified by flow cytometry. Data are presented as means ± SD from three replicates.

DC from pGM-CSF- and FL-treated mice are functionally equivalent in their capacity to stimulate T cell proliferation

pGM-CSF-generated DC were compared with FL-generated DC for their capacity to stimulate the in vitro proliferation of allogeneic $CD4^+$ or $CD8^+$ T cells. Purified splenic DC from FL- or pGM-CSF-treated C57BL/6 mice ($H\text{-}2^b$) were cultured in the presence of purified $CD4^+$ or $CD8^+$ LN T cells from DBA/2 mice ($H\text{-}2^d$). DC from FL- or pGM-CSF-treated mice were functionally equivalent in their capacities to stimulate allogeneic $CD4^+$ or $CD8^+$ T cell proliferation (Fig. 6). We next assessed the capacity of the various DC to stimulate Ag-specific T cell proliferation in vitro. We cultured DC with LN T cells from DO11.10 transgenic mice which express rearranged TCRα and TCRβ genes encoding for a TCR specific for the peptide fragment $OVA_{323–329}$ presented on $I\text{-}A^d$ MHC class II molecules (21). No consistent differences were observed in the capacity of FL- or pGM-CSF-generated DC to present soluble OVA peptide or OVA protein and stimulate the proliferation of DO11.10 T cells (Fig. 7).

$CD11b^{high}CD11c^{high}$ but not $CD11b^{los}CD11c^{high}$ DC expansion is deficient in FL-treated GM-CSFR$\beta^{-/-}$ mice

Although administration of FL in vivo induces the generation of both $CD11b^{high}CD11c^{high}$ and $CD11b^{low}CD11c^{high}$ DC, it is unclear whether this is strictly FL-mediated or due to the combined action of FL and endogenous cytokines. Previous studies have demonstrated marginal changes in DC numbers in GM-CSFR$\beta^{-/-}$ mice, the most significant of these being a 3-fold decrease in DC in the LN (9). To determine whether FL-mediated DC expansion in vivo is dependent on GM-CSF, we treated GM-CSFR$\beta^{-/-}$ mice with FL. Spleen cellularity was increased similarly in FL-treated GM-CSFR$\beta^{-/-}$ and GM-CSFR$\beta^{+/+}$ mice as was the generation of $CD11b^{low}CD11c^{high}$ DC (Table II). However, FL generated fewer $CD11b^{high}CD11c^{high}$ DC in GM-CSFR$\beta^{-/-}$ mice than in GM-CSFR$\beta^{+/+}$ controls (Table II), suggesting that FL-mediated expansion of $CD11b^{high}CD11c^{high}$ DC involves, to some extent, GM-CSF/GM-CSFR signaling. However, because development of $CD11b^{high}CD11c^{high}$ DC was not completely abrogated in GM-CSFR$\beta^{-/-}$ mice, GM-CSFRβ chain signaling is not an absolute requirement for $CD11b^{high}CD11c^{high}$ DC development. The allostimulatory capacity of splenic DC from FL-treated GM-CSFR$\beta^{-/-}$ mice was equivalent to FL-generated splenic DC from GM-CSFR$\beta^{+/+}$ mice, indicating that DC generated with FL in GM-CSFR$\beta^{-/-}$ mice were functionally normal (not shown).

Discussion

Daily administration of a chemically modified form of GM-CSF (pGM-CSF) with an extended pharmacokinetic half-life demonstrates that this cytokine can expand the number of DC in mice. This is consistent with a previous report using GM-CSF-transfected tumor cells (12, 13) but is in contrast to other reports examining either GM-CSF-transgenic mice or systemic treatment with recombinant, unmodified, yeast-derived GM-CSF (10, 11). The discrepancies likely reflect differences in the endogenous levels of GM-CSF reached in GM-CSF-transgenic mice as compared with transfected tumor cells as well as differences between the biological half-life of recombinant GM-CSF as compared with its biochemically modified pGM-CSF counterpart. The availability of a more biologically potent form of GM-CSF allowed for the direct comparison of GM-CSF- and FL-mediated DC expansion in vivo and has revealed several distinctions between GM-CSF and FL.

First, both FL and pGM-CSF generate significant numbers of DC in vivo, but maximal DC numbers are achieved after 5 days of

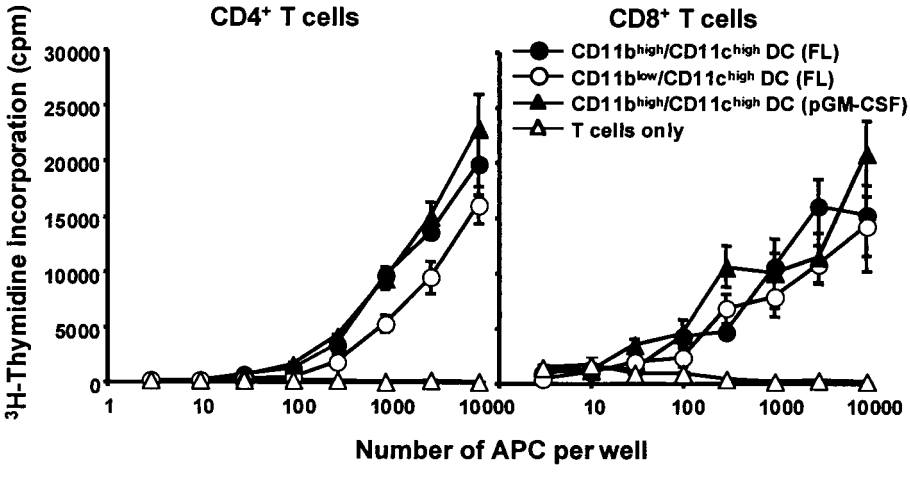

FIGURE 6. DC from pGM-CSF-treated mice are equivalent to FL-generated DC in inducing alloreactive T cell proliferation. Purified splenic DC from pGM-CSF- and FL-treated C57BL/6 mice ($H\text{-}2^b$) were cultured in the presence of purified $CD4^+$ or $CD8^+$ LN T cells from DBA/2 mice ($H\text{-}2^d$), and T cell proliferation was monitored by [^{3}H]thymidine incorporation. Data are presented as the mean ± SEM of triplicate cultures and are representative of three separate experiments. Both panels share the same legend.

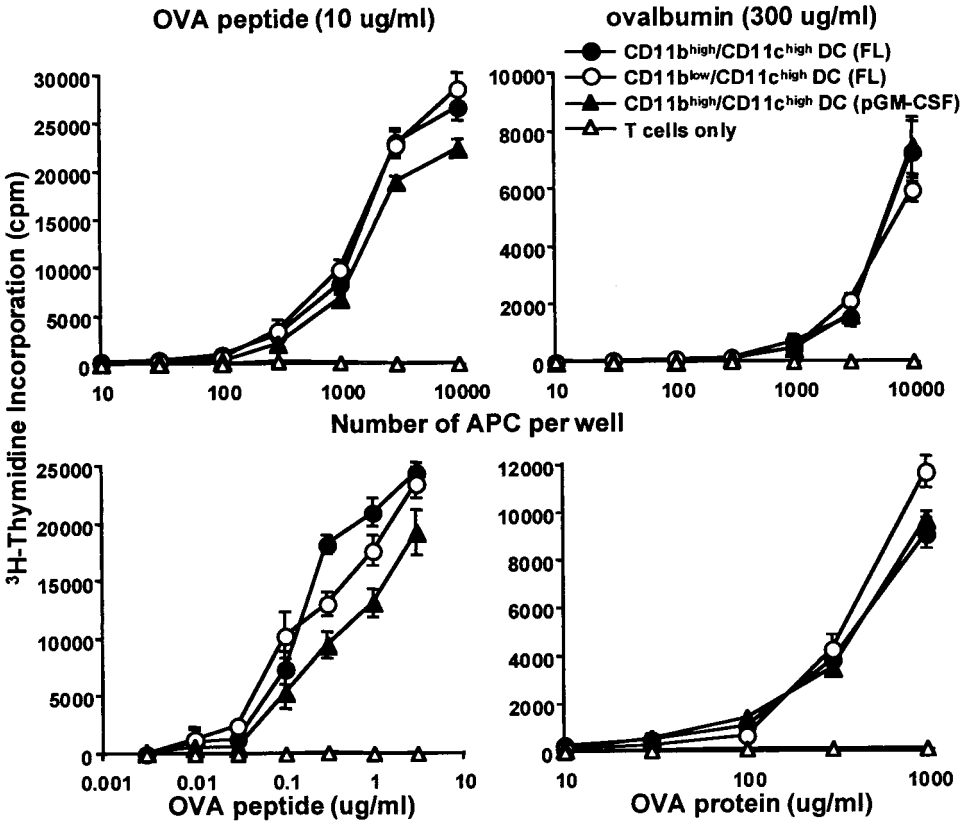

FIGURE 7. CD11b^{high}CD11c^{high} DC from pGM-CSF-treated mice are functionally equivalent to FL-generated DC in inducing Ag-specific T cell proliferation. Splenic DC from pGM-CSF- and FL-treated BALB/c mice (H-2^d) were cultured in the presence of naive CD4$^+$CD62L$^+$ T cells from OVA-TCR-transgenic DO11.10 mice (H-2^d) in the continued presence of OVA peptide or protein. T cell proliferation was monitored by [^{3}H]thymidine incorporation. Data are presented as the means ± SEM of triplicate cultures from one experiment. Similar results were obtained on several occasion except we did always find that pGM-CSF-generated DC were less efficient than FL-generated DC in presentation of ova peptide. All four panels share the same legend.

pGM-CSF treatment, whereas FL requires 9 days treatment to reach maximal DC numbers. Continuous treatment with pGM-CSF causes DC numbers to gradually return to normal levels after 10 days, whereas DC numbers remain elevated in response to continuous treatment with FL for >10 days. It is possible that the more rapid kinetics of DC expansion achieved with pGM-CSF may reflect differences in the differentiation time of the respective precursor cell targets. It is known that the Flt3 receptor is restricted to more primitive progenitor cells and immature myeloid and B-lymphoid precursors, whereas GM-CSF receptor is expressed on more mature myeloid cells including mature monocytes and DC (28–30). Examining DC development in mice sequentially treated with FL and pGM-CSF may shed light on the mechanism of action of these two cytokines.

Second, whereas FL induces the generation of both CD11b^{high}CD11c^{high}CD8α^-, and CD11b^{low}CD11c^{high}CD8α^+ DC, pGM-CSF primarily induces the generation CD11b^{high}CD11c^{high}CD8α^- DC (Fig. 1*A*; Fig. 2), (17). In addition, expansion of CD11b^{low}CD11c^{high}CD8α^+ DC in FL-treated GM-CSFR$\beta^{-/-}$ mice is normal, whereas expansion of CD11b^{high}CD11c^{high}CD8α^- DC is reduced by 50% (Table II).

Table II. *DC subsets from FL-treated GM-CSFR$\beta^{-/-}$ mice*[a]

	Cell Recovery/Spleen ($\times 10^{-6}$)		
	Total cells	CD11b^{high}/ CD11c^{high} DC	CD11b^{low}/ Cd11c^{high} DC
GM-CSFR$\beta^{+/+}$	260 ± 40	21 ± 3	36 ± 6
GM-CSFR$\beta^{-/-}$	220 ± 30	13 ± 3	36 ± 6

[a] Absolute number of cells (mean ± SD) × 10^{-6} of two separate experiments derived from 10 mice/group.

Taken together, these data suggest that GM-CSF minimally influences the development of CD11b^{low}CD11c^{high}CD8α^+ DC. DC can be derived from both myeloid- and lymphoid-committed precursors (5). In the mouse spleen, myeloid-related DC are characterized as CD11b^{high}CD11c^{high}CD8α^- (20, 25, 31). Conversely, it has been proposed that the ontogenic derivation of CD11b^{low}CD11c^{high}CD8α^+ spleen DC is related to thymic DC, which appear to be derived from a lymphoid-committed precursor (32–35). CD11b^{low}CD11c^{high}CD8α^+ spleen DC are phenotypically indistinguishable from thymic DC. The lymphoid origin of CD11b^{low}CD11c^{high}CD8α^+ spleen DC is further supported by findings that i.v. injection of lymphoid-committed precursors results in the exclusive generation of CD11b^{low}CD11c^{high}CD8α^+ DC in both the thymus and spleen (35). Thus, our studies of in vivo administration of pGM-CSF and analysis of FL-treated GM-CSFR$\beta^{-/-}$ mice suggest that GM-CSF plays an important role in the development of CD11b^{high}CD11c^{high}CD8α^- myeloid-related DC but is not essential for the development of the CD11b^{low}CD11c^{high}CD8α^+ putative lymphoid-related spleen DC subset.

Third, DC generated by pGM-CSF differ in the expression of certain surface molecules. DC generated by pGM-CSF uniformly express high levels of the marginal zone marker, 33D1. In contrast, FL-generated, CD11b^{high}CD11c^{high} DC can be subdivided into 33D1$^+$ and 33D1$^-$ subpopulations (Fig. 2) (20). This may indicate that pGM-CSF-generated DC represent a more homogeneous population of CD11b^{high}CD11c^{high} DC than those generated with FL. The biological function of 33D1 on CD11b^{high}CD11c^{high} DC in the marginal zone is not clear but may reflect DC developmental origins (e.g., macrophage/monocyte rather than Langerhans cell). Alternatively, 33D1 expression may relate to DC maturational status and functional role in this location, given that the marginal

zone is a primary entry point for particulate Ag trafficking from the circulation (20, 36). The Ag recognition receptor DEC205 and the lymphoid-related DC marker CD8α are not expressed on pGM-CSF-generated, CD11b^{high}CD11c^{high} DC. This is consistent with previous reports that CD8α and DEC205 are coordinately expressed on CD11b^{low}CD11c^{high} DC within the T cell areas (11, 20, 37, 38). Another difference in surface phenotype between FL- and pGM-CSF-generated CD11b^{high}CD11c^{high} DC is the somewhat higher level of expression of CD1d on pGM-CSF-generated DC. Previously, we have shown a strong correlation between CD1d, DEC205, and CD8α on CD11b^{low}CD11c^{high} DC from FL-treated mice (20). The presence of CD1d on the pGM-CSF-generated, CD11b^{high}CD11c^{high} DC suggests that this marker may not be restricted to CD11b^{low}CD11c^{high} DC. CD1d may play a role in unconventional Ag presentation to specific T cell populations (reviewed in Ref. 39); therefore, the expression of CD1d on pGM-CSF-generated DC may be functionally significant.

Finally, pGM-CSF-generated DC are more efficient at Ag capture and processing than FL-generated DC. The correlation between surface phenotype and functional status of DC has become a widely accepted means of assessing DC maturation, particularly for in vitro-generated DC from monocyte precursors (reviewed in Refs. 4 and 5). The pGM-CSF-generated DC retain a high capacity for Ag capture and processing, a characteristic of immature DC. In contrast, FL-generated splenic DC are comparatively less efficient at this function and therefore appear to represent a functionally more mature DC population (Fig. 3). However, the expression level of costimulatory molecules is quite low in both FL- and pGM-CSF-generated DC, a phenotype consistent with immature DC. Intracellular MHC Class II distribution reveals that both FL- and pGM-CSF-generated, CD11b^{high}CD11c^{high} contain equivalent amounts of intracellular and surface MHC class II. Interestingly, FL-generated, CD11b^{low}CD11c^{high} DC retain the highest levels of intracellular MHC Class II, a phenotype associated with immature DC. Furthermore, both FL- and pGM-CSF-generated DC are efficient stimulators of allogeneic or Ag-specific T cell proliferation in vitro, a hallmark of mature DC (Figs. 6 and 7). DC terminally differentiate when placed in culture with T cells, and thus differences in initial maturation phenotype/function may be obscured by the in vitro culture conditions. Overall, none of the DC populations analyzed display all of the characteristics expected of either mature or immature DC. This is not due to heterogeneity in DC populations because each functional or phenotypic characteristic is expressed homogeneously by the DC populations analyzed. These findings are consistent with our analysis of DC generated in FL-treated human volunteers, which exhibit low Ag capture capacity, low expression of costimulatory molecules and efficient stimulation of T cells (52).

There are several possible explanations for the findings that none of the DC populations analyzed displayed all of the characteristics expected of either mature or immature DC. These include but are not limited to the following. 1) Functional and phenotypic transitions observed during DC maturation may not be synchronously coupled. For example, the down-regulation of Ag capture activity may occur at a different rate or may be initiated at a different phase of the DC maturation program than that of increased costimulatory molecule expression. 2) Cytokines such as GM-CSF or FL may directly or indirectly affect DC function and/or phenotype regardless of maturation. This is supported by findings that GM-CSF can increase Ag capture by DC in vitro (7, 40) and may indicate that the GM-CSF used in these studies imparts the macrophage-like characteristic of active phagocytosis on DC as they develop in vivo. The presence of the high levels of FL or GM-CSF used in these studies could also induce aberrant cell development or maturation. 3) The DC generated by FL and pGM-CSF represent an intermediate maturation stage. It is likely that further maturation of FL- or pGM-CSF DC will be induced by specific maturation signals. DC maturation has been shown to be induced after exposure to several classes of signals: proinflammatory mediators such as IL-1β, IL-6, TNF-α, PGE_2, and IFN-α (41–44); T-cell derived signals such as CD40 ligand (45, 46); and pathogen-derived signals such as LPS, viral dsDNA, and bacterial CpG DNA (47, 48).

Due to the capacity of DC to modulate immune responses, they have been under clinical investigation as cellular vaccine adjuvants (49, 50). Given that DC represent a diverse family of leukocytes, it is as yet unclear which DC populations are the most appropriate for the generation of long lasting and clinically effective immune responses in vivo. Furthermore, the effective delivery of vaccines will also depend on matching the form of Ag (peptide, protein, and cDNA) with the functional capacity and maturation status of the DC population used. The present study provides a foundation for evaluating the use of FL and pGM-CSF in generating DC in vivo and for optimizing their clinical utility.

Acknowledgments

We thank Dr. M. Jenkins for the gift of the DO11.10-transgenic mice and for helpful advice; Daniel Hirschstein, Steve Braddy, Alan Alpert, and Franke Batte for their assistance with flow cytometry; Anne Aumell for editorial assistance; Gary Carlton for graphics assistance; and Drs. Eric Butz, Thibaut DeSmedt, Neil Fanger, and Laurent Galibert for insightful discussions.

References

1. Steinman, R. M. 1991. The dendritic cell system and its role in immunogenicity. *Annu. Rev. Immunol. 9:271.*
2. Metlay, J. P., M. D. Witmer-Pack, R. Agger, M. T. Crowley, D. Lawless, and R. M. Steinman. 1990. The distinct leukocyte integrins of mouse spleen dendritic cells as identified with new hamster monoclonal antibodies. *J. Exp. Med. 171: 1753.*
3. Austyn, J. M. 1996. New insights into the mobilization and phagocytic activity of dendritic cells. *J. Exp. Med. 183:1287.*
4. Mellman, I., S. J. Turley, and R. M. Steinman. 1998. Antigen processing for amateurs and professionals. *Trends Cell Biol. 8:231.*
5. Banchereau, J., and R. M. Steinman. 1998. Dendritic cells and the control of immunity. *Nature 392:245.*
6. Caux, C., C. Massacrier, B. Vanbervliet, B. Dubois, I. Durand, M. Cella, A. Lanzavecchia, and J. Banchereau. 1997. CD34$^+$ hematopoietic progenitors from human cord blood differentiate along two independent dendritic cell pathways in response to granulocyte-macrophage colony-stimulating factor plus tumor necrosis factor α. II. Functional analysis. *Blood 90:1458.*
7. Sallusto, F., M. Cella, C. Danieli, and A. Lanzavecchia. 1995. Dendritic cells use macropinocytosis and the mannose receptor to concentrate macromolecules in the major histocompatibility complex class II compartment: downregulation by cytokines and bacterial products. *J. Exp. Med. 182:389.*
8. Pierre, P., S. J. Turley, E. Gatti, M. Hull, J. Meltzer, A. Mirza, K. Inaba, R. M. Steinman, and I. Mellman. 1997. Developmental regulation of MHC class II transport in mouse dendritic cells. *Nature 388:787.*
9. Vremec, D., G. J. Lieschke, A. R. Dunn, L. Robb, D. Metcalf, and K. Shortman. 1997. The influence of granulocyte/macrophage colony-stimulating factor on dendritic cell levels in mouse lymphoid organs. *Eur. J. Immunol. 27:40.*
10. Metcalf, D., K. Shortman, D. Vremec, S. Mifsud, and L. Di Rago. 1996. Effects of excess GM-CSF levels on hematopoiesis and leukemia development in GM-CSF/*max* 41 double transgenic mice. *Leukemia 10:713.*
11. Maraskovsky, E., K. Brasel, M. Teepe, E. R. Roux, S. D. Lyman, K. Shortman, and H. J. McKenna. 1996. Dramatic increase in the numbers of functionally mature dendritic cells in Flt3 ligand-treated mice: multiple dendritic cell subpopulations identified. *J. Exp. Med. 184:1953.*
12. Hanada, K., R. Tsunoda, and H. Hamada. 1996. GM-CSF-induced in vivo expansion of splenic dendritic cells and their strong costimulation activity. *J. Leukocyte Biol. 60:181.*
13. Bronte, V., D. B. Chappell, E. Apolloni, A. Cabrelle, M. Wang, P. Hwu, and N. P. Restifo. 1999. Unopposed production of granulocyte-macrophage colony-stimulating factor by tumors inhibits CD8$^+$ T cell responses by dysregulating antigen-presenting cell maturation. *J. Immunol. 162:5728.*
14. Dranoff, G., E. Jaffee, A. Lazenby, P. Golumbek, H. Levitsky, K. Brose, V. Jackson, H. Hamada, D. Pardoll, and R. C. Mulligan. 1993. Vaccination with irradiated tumor cells engineered to secrete murine granulocyte-macrophage colony-stimulating factor stimulates potent, specific, and long-lasting anti-tumor immunity. *Proc. Natl. Acad. Sci. USA 90:3539.*

15. Chiodoni, C., P. Paglia, A. Stoppacciaro, M. Rodolfo, M. Parenza, and M. P. Colombo. 1999. Dendritic cells infiltrating tumors cotransduced with granulocyte/macrophage colony-stimulating factor (GM-CSF) and CD40 ligand genes take up and present endogenous tumor-associated antigens, and prime naive mice for a cytotoxic T lymphocyte response. *J. Exp. Med. 190:125.*
16. Curiel-Lewandrowski, C., K. Mahnke, M. Labeur, B. Roters, W. Schmidt, R. D. Granstein, T. A. Luger, T. Schwarz, and S. Grabbe. 1999. Transfection of immature murine bone marrow-derived dendritic cells with the granulocyte-macrophage colony-stimulating factor gene potently enhances their in vivo antigen-presenting capacity. *J. Immunol. 163:174.*
17. Pulendran, B., J. L. Smith, G. Caspary, K. Brasel, D. Pettit, E. Maraskovsky, and C. R. Maliszewski. 1999. Distinct dendritic cell subsets differentially regulate the class of immune response in vivo. *Proc. Natl. Acad. Sci. USA 96:1036.*
18. Delgado, C., G. E. Francis, and D. Fisher. 1992. The uses and properties of PEG-linked proteins. *Crit. Rev. Ther. Drug Carrier Syst. 9:249.*
19. Shurin, M. R., P. P. Pandharipande, T. D. Zorina, C. Haluszczak, V. M. Subbotin, O. Hunter, A. Brumfield, W. J. Storkus, E. Maraskovsky, and M. T. Lotze. 1997. FLT3 ligand induces the generation of functionally active dendritic cells in mice. *Cell. Immunol. 179:174.*
20. Pulendran, B., J. Lingappa, M. K. Kennedy, J. Smith, M. Teepe, A. Rudensky, C. R. Maliszewski, and E. Maraskovsky. 1997. Developmental pathways of dendritic cells in vivo: distinct function, phenotype and localization of dendritic cell subsets in FLT3 ligand-treated mice. *J. Immunol. 159:2222.*
21. Murphy, K. M., A. B. Heimberger, and D. Y. Loh. 1990. Induction by antigen of intrathymic apoptosis of $CD4^+CD8^+TCR^{lo}$ thymocytes in vivo. *Science 250: 1720.*
22. Robb, L., C. C. Drinkwater, D. Metcalf, R. Li, F. Kontgen, N. A. Nicola, and C. G. Begley. 1995. Hematopoietic and lung abnormalities in mice with a null mutation of the common β subunit of the receptors for granulocyte-macrophage colony-stimulating factor and interleukins 3 and 5. *Proc. Natl. Acad. Sci. USA 92:9565.*
23. Price, V., D. Mochizuki, C. J. March, D. Cosman, M. C. Deeley, R. Klinke, W. Clevenger, S. Gillis, P. Baker, and D. Urdal. 1987. Expression, purification and characterization of recombinant murine granulocyte-macrophage colony-stimulating factor and bovine interleukin-2 from yeast. *Gene 55:287.*
24. Lynch, D. H., C. Jacobs, D. DuPont, J. Eisenman, D. Foxworthe, U. Martin, R. E. Miller, E. Roux, D. Liggitt, and D. E. Williams. 1992. Pharmacokinetic parameters of recombinant mast cell growth factor (rMGF). *Lymphokine Cytokine Res. 11:233.*
25. Vremec, D., and K. Shortman. 1997. Dendritic cell subtypes in mouse lymphoid organs: cross-correlation of surface markers, changes in incubation, and differences among thymus, spleen, and lymph nodes. *J. Immunol. 159:565.*
26. Garrett, W. S., and I. Mellman. 1999. *Studies of Endocytosis*. Academic Press, San Diego, CA.
27. Mellman, I. 1996. Endocytosis and molecular sorting. *Annu. Rev. Cell Dev. Biol. 12:575.*
28. Rasko, J. E., D. Metcalf, M. T. Rossner, C. G. Begley, and N. A. Nicola. 1995. The flt3/flk-2 ligand: receptor distribution and action on murine haemopoietic cell survival and proliferation. *Leukemia 9:2058.*
29. Williams, D. E., D. C. Bicknell, L. S. Park, J. E. Straneva, S. Cooper, and H. E. Broxmeyer. 1988. Purified murine granulocyte/macrophage progenitor cells express a high-affinity receptor for recombinant murine granulocyte/macrophage colony-stimulating factor. *Proc. Natl. Acad. Sci. USA 85:487.*
30. Wognum, A. W., M. O. de Jong, and G. Wagemaker. 1996. Differential expression of receptors for hemopoietic growth factors on subsets of $CD34^+$ hemopoietic cells. *Leuk Lymphoma 24:11.*
31. Shortman, K., and C. Caux. 1997. Dendritic cell development: multiple pathways to nature's adjuvants. *Stem Cells 15:409.*
32. Vremec, D., M. Zorbas, R. Scollay, D. J. Saunders, C. F. Ardavin, L. Wu, and K. Shortman. 1992. The surface phenotype of dendritic cells purified from mouse thymus and spleen: investigation of the CD8 expression by a subpopulation of dendritic cells. *J. Exp. Med. 176:47.*
33. Ardavin, C., L. Wu, C.-L. Li, and K. Shortman. 1993. Thymic dendritic cells and T cells develop simultaneously in the thymus from a common precursor population. *Nature 362:761.*
34. Galy, A., M. Travis, D. Cen, and B. Chen. 1995. Human T, B, natural killer, and dendritic cells arise from a common bone marrow progenitor cell subset. *Immunity 3:459.*
35. Wu, L., C.-L. Li, and K. Shortman. 1996. Thymic dendritic cell precursors: relationship to the T lymphocyte lineage and phenotype of the dendritic cell progeny. *J. Exp. Med. 184:903.*
36. Inaba, K., W. J. Swiggard, M. Inaba, J. Meltzer, A. Mirza, T. Sasagawa, M. C. Nussenzweig, and R. M. Steinman. 1995. Tissue distribution of the DEC-205 protein that is detected by the monoclonal antibody NLDC-145. I. Expression on dendritic cells and other subsets of mouse leukocytes. *Cell. Immunol. 163:148.*
37. Inaba, K., M. Pack, M. Inaba, H. Sakuta, F. Isdell, and R. M. Steinman. 1997. High levels of a major histocompatibility complex II-self peptide complex on dendritic cells from the T cell areas of lymph nodes. *J. Exp. Med. 186:665.*
38. Salomon, B., J. L. Cohen, C. Masurier, and D. Klatzmann. 1998. Three populations of mouse lymph node dendritic cells with different origins and dynamics. *J. Immunol. 160:708.*
39. Blumberg, R. S., D. Gerdes, A. Chott, S. A. Porcelli, and S. P. Balk. 1995. Structure and function of the CD1 family of MHC-like cell surface proteins. *Immunol. Rev. 147:5.*
40. Lutz, M. B., C. U. Assmann, G. Girolomoni, and P. Ricciardi-Castagnoli. 1996. Different cytokines regulate antigen uptake and presentation of a precursor dendritic cell line. *Eur. J. Immunol. 26:586.*
41. Rieser, C., G. Böck, H. Klocker, G. Bartsch, and M. Thurnher. 1997. Prostaglandin E_2 and tumor necrosis factor α cooperate to activate human dendritic cells: synergistic activation of interleukin 12 production. *J. Exp. Med. 186:1603.*
42. Jonuleit, H., U. Kühn, G. Müller, K. Steinbrink, L. Paragnik, E. Schmitt, J. Knop, and A. H. Enk. 1997. Pro-inflammatory cytokines and prostaglandins induce maturation of potent immunostimulatory dendritic cells under fetal calf serum-free conditions. *Eur. J. Immunol. 27:3135.*
43. Reddy, A., M. Sapp, M. Feldman, M. Subklewe, and N. Bhardwaj. 1997. A monocyte conditioned medium is more effective than defined cytokines in mediating the terminal maturation of human dendritic cells. *Blood 90:3640.*
44. Luft, T., K. C. Pang, E. Thomas, P. Hertzog, D. N. Hart, J. Trapani, and J. Cebon. 1998. Type I IFNs enhance the terminal differentiation of dendritic cells. *J. Immunol. 161:1947.*
45. Koch, F., U. Stanzl, P. Jennewein, K. Janke, C. Heufler, E. Kampgen, N. Romani, and G. Schuler. 1996. High level IL-12 production by murine dendritic cells: upregulation via MHC class II and CD40 molecules and downregulation by IL-4 and IL-10. *J. Exp. Med. 184:741.*
46. Cella, M., D. Scheidegger, K. Palmer-Lehmann, P. Lane, A. Lanzavecchia, and G. Alber. 1996. Ligation of CD40 on dendritic cells triggers production of high levels of interleukin-12 and enhances T cell stimulatory capacity: T-T help via APC activation. *J. Exp. Med. 184:747.*
47. Cella, M., M. Salio, Y. Sakakibara, H. Langen, I. Julkunen, and A. Lanzavecchia. 1999. Maturation, activation, and protection of dendritic cells induced by double-stranded RNA. *J. Exp. Med. 189:821.*
48. Hartmann, G., G. J. Weiner, and A. M. Krieg. 1999. CpG DNA: a potent signal for growth, activation, and maturation of human dendritic cells. *Proc. Natl. Acad. Sci. USA 96:9305.*
49. Schuler, G., and R. M. Steinman. 1997. Dendritic cells as adjuvants for immune-mediated resistance to tumors. *J. Exp. Med. 186:1183.*
50. Nestle, F. O., S. Alijagic, M. Gilliet, Y. Sun, S. Grabbe, R. Dummer, G. Burg, and D. Schadendorf. 1998. Vaccination of melanoma patients with peptide- or tumor lysate-pulsed dendritic cells. *Nat. Med. 4:328.*
51. McKenna, H. J., K. L. Stocking, R. E. Miller, K. Brasel, T. De Smedt, E. Maraskovsky, C. R. Maliszewski, D. H. Lynch, J. Smith, B. Pulendran, E. R. Roux, M. Teepe, S. D. Lyman, and J. J. Peschon. 2000. Mice lacking Flt3 ligand have deficient hematopoiesis affecting hematopoietic progenitor cells, dendritic cells and natural killer cells. *Blood. In press.*
52. Maraskovsky E., E. Daro, E. Roux, M. Teepe, C. R. Maliszewski, J. Hoek, D. Caron, M. E. Lebsack, and H. J. McKenna. 2000. In vivo generation of human dendritic cell subsets by Flt3 ligand. *Blood. In press.*